Talanta 107 (2013) 176–182

Contents lists available at SciVerse ScienceDirect

Talanta

journal homepage: www.elsevier.com/locate/talanta

Graphene oxide as nanocarrier for sensitive electrochemical immunoassay of clenbuterol based on labeling amplification strategy

Yanjun Lai, Jing Bai, XinHao Shi, Yanbo Zeng, Yuezhong Xian *, Jie Hou, Litong Jin *

Department of Chemistry, East China Normal University, Shanghai 200062, PR China

ARTICLE INFO

Article history:
Received 2 August 2012
Received in revised form
1 January 2013
Accepted 4 January 2013
Available online 16 January 2013

Keywords:
Electrochemical immunosensor
Clenbuterol
Graphene oxide
Gold nanoparticles
Glucose oxide
Prussian blue

ABSTRACT

A novel electrochemical immunosensor for sensitive detection of clenbuterol (CLB) is fabricated using glucose oxidase (GOD)-functionalized grahene oxide (GO) nanocomposites to label CLB. The immunosensor was constructed by layer-by-layer assembly colloidal prussian blue (PB), multiwalled carbon nanotubes (MWCNTs) and CLB antibodies (Abs) on a glassy carbon electrode (GCE). In this competitive immunoassay system, PB acts as the redox mediator to reduce H_2O_2 originated from the catalyst cycle of GOD. The high ratio of GOD to GO effectively amplified the signal for this competitive-type immunoassay. Under optimized conditions, the immunosensor shows a wide linear range from 0.5 to 1000 ng/mL with a low detection limit of 0.25 ng/mL. The dual signal amplification of GOD-functionalized GO nanocomposites as a label is promising to be applied to design other sensitive immunosenseors.

1. Introduction

Clenbuterol (CLB), as a β-agonist, can reduce stress symptoms and asthma, leading to its widespread use in the treatment of human depression and pulmonary diseases [1]. However, due to its unique function of promoting fat consumption [2,3], some illegal producers often add CLB at high doses to the feed of livestocks to improve the production of lean meat. Large amounts of CLB residues in the produced meat associate with serious side effects and food poisoning [4]. For this reason, several countries have forbidden the use of CLB as growth promoter. In the past few years, the illegal misuse of CLB has caused several serious food poisoning tragedies in China, Italy and France [5,6]. It is followed that establishing a simple, rapid and sensitive method for the determination of CLB is extremely important to ensure food safety. At present, various methods have been reported for CLB detection including high-performance liquid chromatography [7,8], gas chromatography—mass spectrometry [9,10], capillary electrophoresis [11], enzyme-linked immunosorbent assay [12,13] and immunosensor based on surface plasmon resonance [14].

Although these methods for the determination of CLB are very promising due to high sensitivity and selectivity, most of them suffer from several disadvantages such as expensive instruments, complicated operating processes. Electrochemical immunosensors have attracted considerable attentions since they not only enjoy the high specificity of immunoassay, but also feature the sensitivity and low expenses of electrochemical systems. So far, only few electrochemical immunosensors [15–17] are constructed for the determination of CLB. It may be attributed to that lots of electrochemical immunosensors are based on the embarrassment of electron transfer of the electrochemical mediator in solutions caused by macrobiomolecules, but CLB, as a small molecular, cannot have significant embarrassment effect on the electron transfer. Therefore, it is a challenge to improve the sensitivity and stability for the determination of CLB with a lower detection limit using electrochemical immunosensors.

In order to enhance the sensitivity, many nanomaterials have been applied to construct electrochemical immunosensors. The functions of these nanomaterials can be divided into two sorts: (1) metal and semiconductor nanoparticles are directly used as electroactive labels to amplify the electrochemical responses [18,19], (2) nanomaterials, with large surface areas, are used as carriers to load electroactive species or enzyme for the amplification of the detectable signal [20,21]. Carbon nanotubes [22,23], carbon nanospheres [24], silica nanoparticles [25] and carboxylated magnetic beads [26] have been used as carriers of electroactive species or enzymes for signal amplification. Graphene oxide (GO), a novel one-atom thick and two-dimensional graphitic carbon system with abundant oxygen functional groups, has attracted increasing attentions in recent years due to unique physical and chemical properties. GO has potential applications in

* Corresponding authors. Tel.: 86-21-62232627; fax: 86-21-62232627.
E-mail addresses: yzxian@chem.ecnu.edu.cn (Y. Xian), ltjin@chem.ecnu.edu.cn (L. Jin).

0039-9140/$ - see front matter © 2013 Elsevier B.V. All rights reserved.
http://dx.doi.org/10.1016/j.talanta.2013.01.002

sensors, nanoelectronic devices and nanomaterials [27–30]. According to previous reports [30–33], the loading ratio of GO could reach 200%, much higher than that of other nanocarriers. Based on the high loading ratio, good biocompatibility, and physiological stability, GO can be used as efficient nanocarriers in electrochemical immunoassay system. Recently, Du's group [34] reported an electrochemical immunosensor based on multi-enzyme amplification strategy for ultrasensitive detection of phosphorylated p53 at Ser392 using GO as a nanocarrier. The immunosensor achieves higher sensitivity and lower detection limit than that of the traditional sandwich electrochemical immunosensors.

Gold nanoparticles (AuNPs) are well known as conductive and biocompatible labels for electrochemical signal amplification. So AuNPs decorated GO nanocomposite (AuNPs/GO) is very promising for electrochemical biosensors for it has large surface area to volume ratio, but better electrical conductivity than GO. Besides, several researches have revealed that AuNPs can effectively absorb biomolecules including enzymes [35], antibodies [22] as well as maintaining their bioactivity. Recently, Izquierdo's group [36] found CLB can be absorbed on the surface of AuNPs by electrostatic interaction or coordination bond at different pHs. Our work is motivated by utilizing AuNPs/GO as nanocarrier to co-immobilize glucose oxidase (GOD) and CLB simultaneously, yielding GOD/GO/AuNPs-CLB (Fig. 1A). AuNPs/GO was prepared by electrostatic interaction using positive (poly-diallyldimethylammonium chloride) (PDDA) as a linker. The electrochemical immunosensors was constructed by layer-by-layer assembly colloidal prussian blue (PB), multiwalled carbon nanotubes (MWCNTs), and CLB antibodies (Abs) on a glassy carbon electrode (GCE) (Fig. 1B). Herein, the PB acts as electron transfer mediator to catalyze reduction of H_2O_2 produced in a GOD directed enzyme reaction [22]. The MWCNTs with abundant carboxyl groups can provide effective scaffolds for the attachment of Abs. Through competitive immuno-recognition, GOD was immobilized onto GCE via the immuno-reaction of GOD/GO/AuNPs-CLB with Abs on the electrode. Electrochemical detection of enzymatic products is performed in the presence of glucose as shown in Fig. 1C. The enzymatic cycle with PB dually amplifies the electrochemical signal. Therefore, a highly sensitive and selective electrochemical immunosensor is developed for CLB with a low detection limit. Moreover, the stability, reproducibility and accuracy of the proposed method are all very satisfactory and suitable for the determination of CLB in real feed samples.

2. Experimental section

2.1. Reagents

CLB, bovine serum albumin (BSA), and chitosan (CS, ≥85% deacetylation), GOD (10,000 units/g, from Aspergillus niger), PDDA (20% w/w in water, MW: 200,000–350,000), 1-(3-(Dimethylamino)-propyl)-3-ethylcarbodiimide hydrochloride (EDC) and N-hydroxysulfo-succinimide (NHS) were all obtained from Sigma-Aldrich Chemical Co. (Shanghai, China) and were used as received. Mouse monoclonal CLB Abs (85%, 8.4 mg/mL, ELISA IC50 0.6 ppb) was purchased from Ucando Biotechnology Co. (Guangzhou, China). MWCNTs (diameter 60–100 nm) were obtained from nanotechnology Co. (Shenzhen, China). Graphite powder (99.95%, 325 mesh) was obtained from Alfa Aesar. All other chemicals were of analytical grade. Phosphate buffered saline (PBS, 0.05 M) with different pH was prepared by mixing the stock solutions of KH_2PO_4 and Na_2HPO_4. The washing buffer was PBS (0.05 M, pH 7.0) containing 0.05% (w/v) Tween 20 (PBST). Blocking solution was 2% (w/v) BSA containing 0.05% Tween 20. All water used was double-deionized water (Milli-Q, Millipore Corporation, Bedford, MA).

2.2. Apparatus

Differential pulse voltammetry (DPV) and electrochemical impedance spectroscopy (EIS) were carried out on CHI 660A electrochemical workstation (CHI, USA) with a conventional three-electrode system, a modified GCE as the working electrode, an Ag/AgCl electrode as the reference electrode and a platinum electrode as the counter electrode. Transmission electron microscopy (TEM) was carried out on a JEOL JEM-2010 (JEOL, Japan). Surface morphological images were taken by a HITACHI S-4800

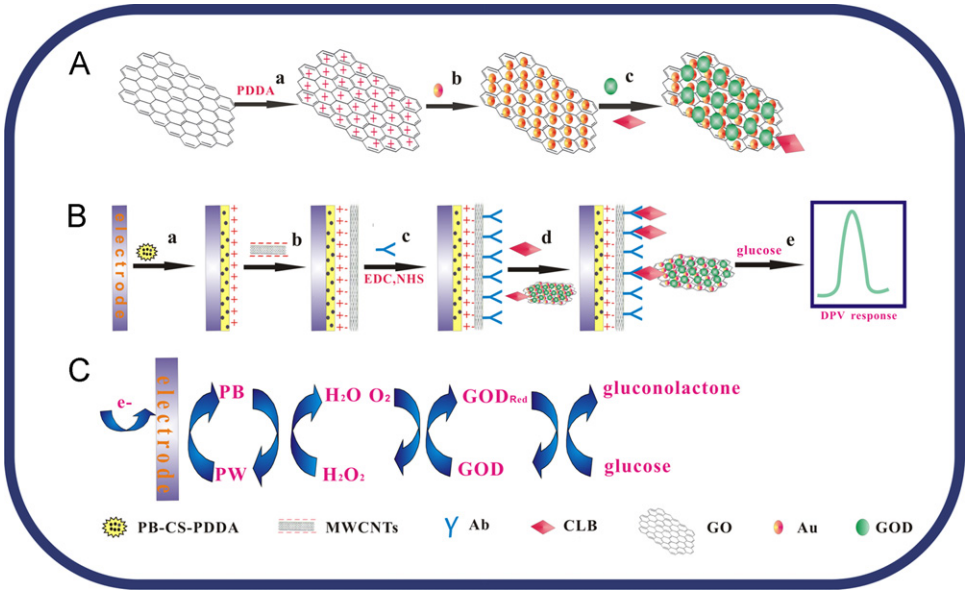

Fig. 1. Schematic representation of (A) preparation procedure of GOD/AuNPs/GO-CLB. (a) formation of PDDA-GO, (b) assembly of AuNPs on PDDA-GO and (c) co-immobilization of GOD and CLB on AuNPs/GO. (B) Construction of immunosensor and competitive electrochemical immunoassay. (a) Formation of a PB-CS-PDDA membrane on GCE, (b) modification with MWCNTs, (c) immobilization of Abs on the modified GCE, (d) competitive immunoreation of CLB in GOD/AuNPs/GO-CLB and in analyte with Abs on the modified GCE and (e) electrochemical measurements of the incubated immunosensor in 10 mM glucose solution. (C) Electrochemical response mechanism of the immunosensor.

scanning electronic microscopy (Hitachi Co. Ltd., Tokyo, Japan). UV–visible spectra were obtained on a Cary 500 UV–vis–NIR spectrometer (Varian, USA). Microwave-irradiated synthesis of AuNPs was operated using refitted microwave oven (Shanghai Xintuo Microwave Instruments Co. Ltd, China). Zeta-potential measurements were conducted with a Zetasizer NanoZS (Malvern Instruments).

2.3. Preparation of GOD/AuNPs/GO-CLB

First, AuNPs with an average diameter of 13 nm were prepared by the microwave method reported by Xu with a slight modification [37]. Briefly, a rockered flask with 50 mL of 0.02% $HAuCl_4$ solution was placed into the microwave oven to be heated (800 W) for 60 s. Subsequently, 2.5 mL 1% trisodium citrate solution was quickly added to the above boiling solution. Then the mixed solution was exposed to microwave radiation (800 W) for 120 s. The color of the mixed solution changed from colorless to purple, then quickly to wine red, indicating the formation of AuNPs, and the final concentration of AuNPs was determined as 5.71×10^{-4} M. The preparation of the GOD/AuNPs/GO-CLB is shown in Fig. 1A. Firstly, GO was prepared from graphite powders by the Hummers method [38]. Next, 5 mL GO dispersion (0.5 mg/mL) was mixed with 10 mL 1% PDDA aqueous solution and sonicated for 2 h and a homogeneous light yellow solution was obtained. Residual PDDA polymer was removed by high-speed centrifugation, and the material was thrice washed with water to obtain PDDA functionalized GO (PDDA-GO), which was further redispersed into 2.5 mL water with mild sonication for usage [39]. To conjugate with AuNPs, 0.5 mL of above-synthesized PDDA-GO colloidal solution was mixed with 1 mL as-prepared AuNPs solution and sonicated for 30 min. After centrifugation, the colorless supernatant was discarded and the purple red AuNPs/GO was washed with water and redispersed in 1 mL of 50 mM pH 9.0 Tris–HCl solution. At room temperature, 125 μL of 2 mg/mL GOD and 5 μL of 1 mg/mL CLB (PBS 7.0) were added to 0.5 mL of above-mentioned AuNPs/GO dispersion. The mixture was gently mixed overnight and centrifuged at 2000 rpm for 15 min. After centrifugation, the obtained precipitate was GOD/AuNPs/GO-CLB. This bioconjugate was washed with washing buffer and resuspended in 1 mL of PBST containing 0.2% BSA as the assay solution (the final ratios of GO and AuNPs were 0.25 mg/mL and 2.85×10^{-4} M, respectively). Prior to use, this solution was 10-fold diluted with PBST.

2.4. Preparation of immunosensor

Nanosized PB colloid protected by PDDA and CS (PB-PDDA-CS) was prepared based on the report of Ju's group [22]. Briefly, at room temperature, 4 mL of 0.025 M $K_3[Fe(CN)_6]$ solution was slowly mixed with 16 mL solution containing 6.25 mM $FeCl_2 \cdot 4H_2O$, 0.4% PDDA, and 0.15 wt% CS (1% HAC solution) under vigorous stirring. Upon mixing, the corresponding solution gradually turned dark blue, indicating the formation of colloidal PB-PDDA-CS. MWCNTs were treated with 3:1 H_2SO_4/HNO_3 in sonication for 4 h. The resulting dispersion was filtered and washed repeatedly with water until pH was about 7.0. This procedure shortened MWCNTs, removed metallic and carbonaceous impurities and generated carboxylate groups on the MWCNTs surface.

The preparation of the immunosensor was illustrated in Fig. 1B. Firstly, 1.0 μL of the resulting PB-PDDA-CS stock solution was dropped on GCE, which was previously pretreated for 2 min at an anodic potential of 1.3 V in 0.1 M H_2SO_4. After drying in air, 2.0 μL of 1 mg/mL MWCNTs dispersed in DMF was cast on GCE and dried under the infrared lamp. Then, 10 μL 400 mM EDC and NHS mixed solution was placed onto the surface of working electrode and activated for 40 min. Rinsed with PBS and PBST for three times, the electrode was incubated with 0.05 mg/mL Abs for 1 h at 37 °C. Subsequently, the resulting electrode was washed three times with PBST and PBS (pH 7.0) to remove the physically absorbed Abs and was incubated with blocking solution for 40 min at room temperature. After that, the resulting working electrode was washed with PBST and PBS successively, and then stored in refrigerator at 4 °C for further usage.

2.5. Preparation of animal feed samples

The preparation of feed samples was in accordance with previous report [16]. A 5 g sample of finely ground swine feed spiked with CLB, was accurately weighed and added into a 50 mL polytetra-fluoroethylene tube, and then 40 mL of freshly prepared phosphate acid–methanol extraction solution (0.2 M) was added. After shaking for 30 min, the mixture was centrifuged at 3000 rpm for 10 min. The supernatant was placed into a 100 mL volumetric flask, and the residuals were extracted using 40 and 20 mL of the same extraction solution twice respectively. The supernatant was collected and diluted into 100 mL with the extraction solution. A 1 mL aliquot of the supernatant was decanted into a 5 mL tube and the solution was evaporated under a stream of nitrogen in a water bath at 55 °C. The extract was redispersed in 5 mL PBS for electrochemical analysis.

2.6. Measurement procedure

To carry out the competitive immunoreation, 3 μL of 1:10 diluted GOD/AuNPs/GO-CLB bioconjugate was stirred with 7 μL CLB solution of various concentrations. The mixed solution was dropped onto the surface of the immmosensor and incubated for 50 min at 37 °C, followed by washing with PBST and PBS for 3 times. Then, the electrochemical measurements were performed in 10 mL of pH 6.5 PBS containing 10 mM glucose. DPV was performed to record the electrochemical responses for quantitative measurement of CLB. The potential is varied from 400 to −200 mV (vs Ag/AgCl) with pulse amplitude of 50 mV and pulse width of 50 ms.

3. Results and discussion

3.1. Characterization of the GOD/AuNPs/GO-CLB

Recent research has indicated that GO with abundant oxygen functional groups can be used as carriers to load numerous enzymes [40]. In this work, the GO was prepared by conventional Hummer's method. The obtained GO shows monolayer flakelike shape (Fig. 2A) and good water solubility. While PDDA-GO was formed, the negatively charged AuNPs could be attached compactly and uniformly on the surface of the GO through electrostatic action (Fig. 2B). The uniformly distributed AuNPs could absorb GOD and CLB to realize the biofunctionalization of GO.

In addition, the effect of electrostatic interaction on the formation of GOD/AuNPs/GO-CLB was further investigated by zeta potential measurement. GO is negatively charged and this negatively charge (−38.7 mV) is due to the ionization of the functional groups like carboxylic acids, that are located on GO platelets [41]. Therefore, the positively charged PDDA can be adsorbed onto GO, and the zeta potential dramatically changed from negative to a very positive value (35.6 mV). After modification with AuNPs, a negatively charged surface (−29.8 mV) of GO-PDDA-Au was obtained, which is due to the adsorption of the negatively charged citrate capped AuNPs on the GO surface [42]. Since the p*K*a2 for CLB is about 9 [43], the interaction between CLB and GO/AuNPs in the absorption reaction (pH=9) is mainly

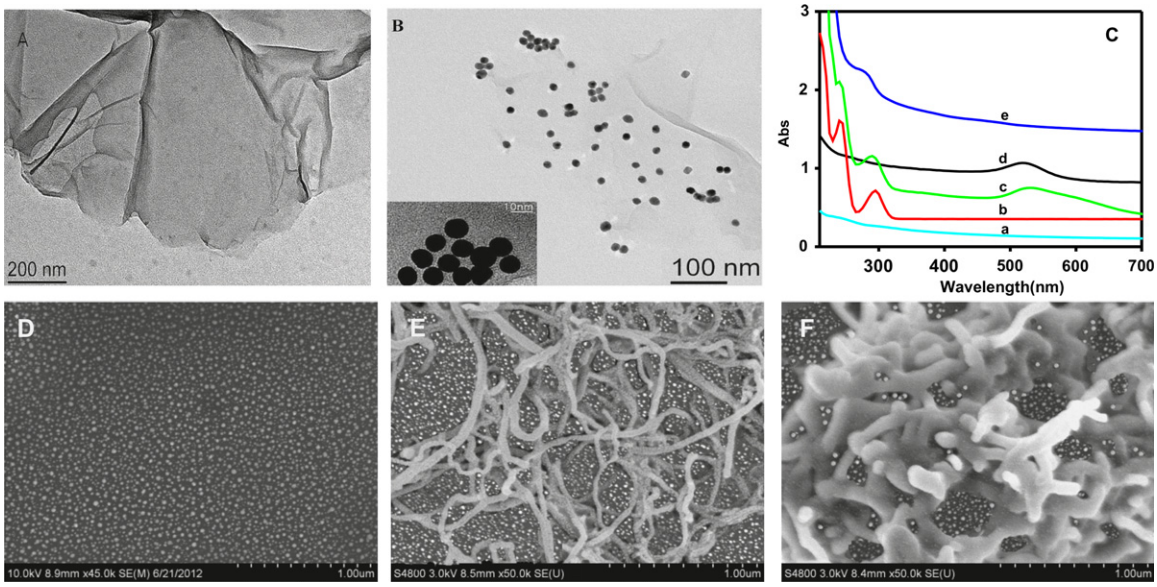

Fig. 2. TEM images of (A) GO and (B) AuNPs/GO, and (C) UV–Vis absorption spectra of (a) GO, (b) CLB, and (c) GOD/AuNPs/GO-CLB, (d) AuNPs, and (e) GOD. SEM images of (D) PB-PDDA-CS/GCE, (E) MWCNTs/PB-PDDA-CS/GCE and (F) Abs/MWCNTs/PB-PDDA-CS/GCE.

caused by coordination bond instead of electrostatic interaction, in accordance with the previous report [36].

The UV–vis characterization was further performed to confirm the formation of GOD/AuNPs/GO-CLB bioconjugate, which was shown in Fig. 2C. No obvious absorption peak is observed for GO (curve a). However, the colloidal solution of AuNPs displays an absorption peak at 519 nm (curve d). After decorating GO with AuNPs, the resulting GOD/AuNPs/GO-CLB nanocomposites show the characteristic peak at 534 nm (curve c), indicating the successful capture of AuNPs. The red shift of resonance wavelength of AuNPs in the nanocomposite results from the interparticle plasmon coupling [44,45]. As for GOD, a distinct absorption peak at 280 nm (curve e) is observed, while CLB shows two characteristic peaks at 240 and 293 nm respectively (curve b). When GOD and CLB were attached onto AuNPs decorated GO, the characteristic peaks for GOD and CLB at 240 and 285 nm (curve c) could be observed. In addition, no absorption peaks were found on the supernatant after centrifugation (data not shown). All results suggest that GOD and CLB could be efficiently attached to the AuNPs/GO.

3.2. Characterizations of the immunosensor

As "artificial peroxidase", PB can electrocatalyze reduction of H_2O_2, which has been extensively used to fabricate glucose biosensors by coimmobilization of GOD [46–48]. Based on the previous report [49], the as-prepared PB colloid shows good dispersibility and stability due to the presence of PDDA and CS. The PDDA-CS protected PB could be directly immobilized on the electrode surface to obtain a stable PB film by virtue of the excellent film forming ability of CS and the electrostatic interaction between cationic PDDA and oxidized pretreatment electrode surface.

Scanning electron microscopy (SEM) was performed to characterize the morphologies of the modified electrode at each step. The results were illustrated in Fig. 2. As shown in Fig. 2D, PB nanoparticles dispersed very well on the electrode, and no particle agglomeration was found, which was due to the protection by PDDA and CS [49]. The diameter of PB nanoparticles is ranged from 5 to 20 nm and the mean sizes are estimated to be 13 nm. When MWCNTs were dropped on the PB modified surface, the electrode surface becomes rough and the diameter of MWCNTs is ranged from 62 to 80 nm as illustrated in Fig. 2E. Upon the immobilization of the Abs, an obvious change of morphology of MWCNT could be observed (Fig. 2F). EIS was chosen to further characterize the process of modification of GCE. It is well-known that the impedance spectra are composed of a semicircle portion and a linear portion. The semicircle diameter at higher frequencies corresponds to the electron-transfer resistance (Ret), and the linear part at lower frequencies reflects the diffusion process. As shown in Fig. 3A. The bare GCE (curve a) displays a small semicircle with a Ret of about 190 Ω at high frequencies. After coated with PDDA-CS protected PB, the electrode shows a higher resistance with a Ret of about 330 Ω (curve b). After further decorated with MWCNTs, the Ret of the modified electrode decreases to about 240 Ω (curve c), indicating that MWCNTs are excellent conductive material and accelerate the electron transfer. Subsequently, while Abs were loaded on the surface of MWCNTs, the Ret increases significantly to 385 Ω, due to the barrier effect of Abs (curve d). It is consistent with the fact that the hydrophobic layer of protein insults the conductive support and hinders the interfacial electron transfer. After incubated with BSA, the Ret is further up to 467 Ω (curve e). Furthermore, the Ret is about 552 Ω while GOD/AuNPs/GO-CLB is bounded onto GCE through antibody–antigen reaction (curve f), indicating the formation of hydrophobic immunocomplex layer which embarrasses the electron transfer.

3.3. Amperometric responses of the immunosensor

The DPVs of the immunosensor under six different conditions in PBS (10 mL, pH 6.5) containing 10 mM glucose are illustrated in Fig. 3B. As shown in curve b, the current peak of BSA/Abs/MWCNTs/PB-PDDA-CS modified GCE (Abs/PB-GCE) in glucose solution appears at 0.153 V, which is corresponding to the reduction of PB. After it is incubated with GOD/AuNPs/GO-CLB, the cathodic current peak increases about 4 times (curve a), which is due to the reduction of H_2O_2 produced in the GOD directed enzymatic catalytic circle. However, when the immunosensor was incubated with a surplus of free CLB, the current response (curve d) reduced slightly compared with that of no incubation (curve b). It indicates that although the formation of

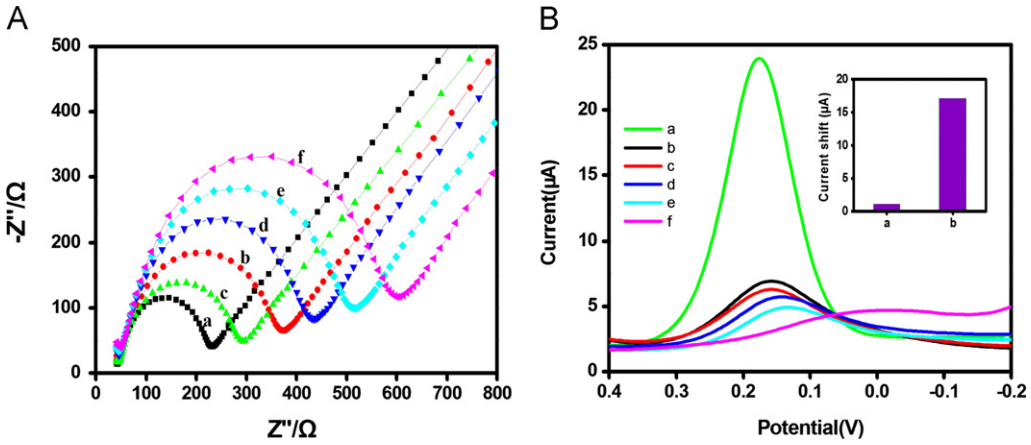

Fig. 3. (A) EIS of (a) bare, (b) PB-PDDA-CS, (c) MWCNTS/PB-PDDA-CS, (d) Ab/MWCNTS/PB-PDDA-CS, (e) BSA/Ab/MWCNTS/PB-PDDA-CS and (f) GOD/AuNPs/GO-CLB/BSA/Ab/MWCNTS/PB-PDDA-CS modified GCE containing 10.0 mM $K_3[Fe(CN)_6]/K_4[Fe(CN)_6]$. (B) DPV responses of (a) Abs/PB GCE captured with GOD/AuNPs/GO-CLB, (b) Abs/PB GCE without incubation, (c) Abs/PB GCE adsorbed with GOD/AuNPs/GO, (d) Abs/PB GCE incubated with a surplus of free CLB, (e) Abs/PB GCE captured with AuNPs/GO-CLB, (f) Abs GCE incubated with GOD/AuNPs/ GO-CLB in PBS (pH 6.5) containing 10 mM glucose. Inset is the cathodic current change for 500 ng/mL CLB without (a) and with (b) GOD/AuNPs/ GO-CLB.

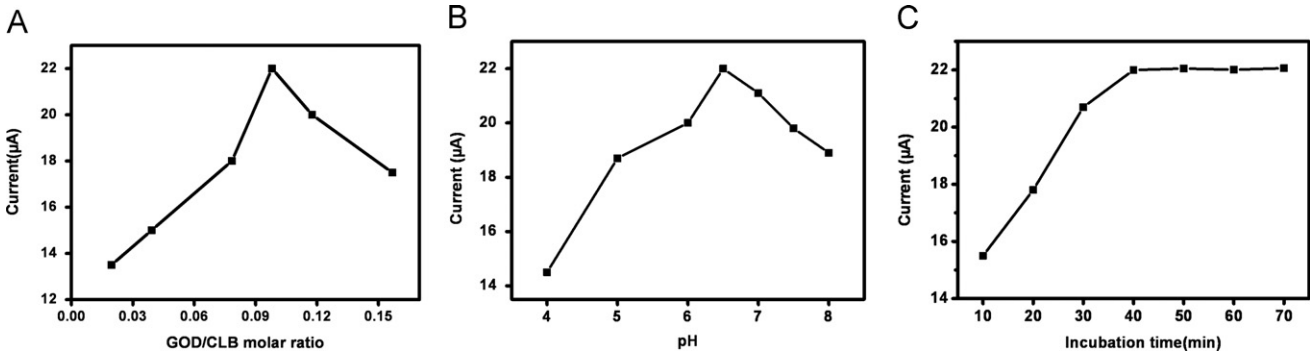

Fig. 4. Effects of (A) molar ratio of GOD to CLB, (B) pH, (C) incubation time on the amperometric responses of electrochemical immunosensor.

the immuno-complex might hinder the electron transfer, the effect is not significant because CLB is small molecule. So signal amplification is very necessary for the sensitive detection of CLB.

The proposed immunosensor is based on dual signal amplification: the first amplification was the GOD directed catalytic circle with the glucose, the second amplification was the PB directed catalytic circle with the H_2O_2 produced in the first circle. In order to better characterize this dual amplification, the cathodic current responses of GOD/AuNPs/GO (curve c) and AuNPs/GO-CLB (curve e) were investigated respectively on Abs/PB-GCE in presence of glucose. The currents are both less than one fifth of that of GOD/AuNPs/GO-CLB (curve a). It indicates that GOD/AuNPs/GO cannot be efficiently immobilized onto GCE because of lacking the antibody–antigen reaction (curve c). As shown in Fig. 3B (e), although AuNPs/GO-CLB can be loaded onto GCE through antibody–antigen action, the electrochemical response is still weak due to the lacking of GOD. In addition, when the immunosensor was constructed without PB (Abs/GCE) and incubated in GOD/AuNPs/GO-CLB, the DPV response is very small (curve f), demonstrating that PB acts as the electron mediator in the enzyme directed catalyst circle (as shown in Fig. 1C). Based on above-mentioned experimental results, we can conclude that only when the GOD/AuNPs/GO-CLB conjugate was linked to the PB modified immunosensor through antibody-antigen reaction, this dual signal amplification can be achieved. Besides, the current peak of GOD/AuNPs/GO (curve c) is little smaller than that of no incubation (curve b), indicating that without the antibody–antigen reaction, the amount of GOD/AuNPs/GO on the GCE is very little and the non-specific absorption was so weak that the catalytic effect of GOD is limited, but the relatively low conductivity of GOD/AuNPs/GO predominantly plays a role instead. Moreover, the current response of AuNPs/GO-CLB (curve e) is weaker than that of just CLB (curve d), also implying lower conductivity of the conjugate.

To demonstrate the dual signal amplification effect for CLB determination, we incubated the immunosensor with CLB directly (10 μL, 500 ng/mL), and the current change with respect to no CLB addition is 1.1 μA (curve a in inset of Fig. 3B). However, as for the immunosensor with GOD/AuNPs/GO-CLB as the tracer, the current change increases to 17.1 μA (curve b in inset of Fig. 3B). It indicates the significant improvement of the sensitivity by dual signal amplification strategy.

3.4. Optimization of conditions for electrochemical detection

In the competitive-type immunoassay, GOD/AuNPs/GO-CLB with a relatively high ratio of GOD to CLB is favorable for the enhancement of electrochemical signal. Therefore, the ratio of GOD/CLB is necessary to be optimized. As shown in Fig. 4A, the amperometric response of the immunosensor reaches the maximum while the molar ratio of GOD/CLB is 0.1. When the molar ratio of GOD/CLB is over 0.1, the electrochemical response is decreased because the excessive GOD molecules can reduce the binding sites of the CLB and lead to the decrease of the amount of functionalized GO onto the immunosensor through the immunoreaction of Abs and CLB. The molar ratio is much lower than those of immunosensors for large molecules by the one-pot method [22,52], for the reason that the immunoreaction of CLB, as a small molecule, is more significantly affected by GOD, as a big molecule.

But the sensitivity of the immunosensor will be improved if GOD and CLB are immobilized onto AuNPs/GO in an order way, which needs further investigation.

The pH and the incubation time are two important parameters in the immuno-reaction. In both optimal experiments, the immunosensor was incubated with 1:10 diluted GOD/AuNPs/GO-CLB at 37 °C. The effect of solution pH on the amperometric response is shown in Fig. 4B. The current increases steeply with the increasing pH from 4.0 to 6.5 and then decreases while the pH is over 6.5. Thus, 0.05 M PBS with pH 6.5 was selected as the detection solution. Fig. 4C displays the amperometric response of the immunosensor increase significantly with the increasing incubation time and then tends to level off after 40 min (Fig. 4C), indicating a saturated binding between the CLB in the nanocomposite and Abs on GCE. Therefore, incubation time is selected as 40 min for the competitive-type immunoassay.

3.5. Analytical performance of immunosensor

Under the optimum conditions, the immunosensor was incubated with 3 μL GOD/AuNPs/GO-CLB and 7 μL CLB standard solutions with different concentrations and the electrochemical response is evaluated. As shown in Fig. 5A, the peak current of the immunosensor decreases with the increasing concentration of CLB. A good linear relationship between the peak current and the logarithm of the CLB concentration is obtained in the ranges from 0.5 to 1000 ng/mL (Fig. 5B). The linear regression equation was $i\ (\mu A) = 15.79 - 3.99 \log C_{CLB}$ (ng/mL) with a correlation coefficient (R) of 0.9979. The detection limit was 0.25 ng/mL at a signal-to-noise ratio of 3, which was defined as the concentration of CLB corresponding to the signal which equals to the zero signal minus three times the standard deviation (R). In this system, the zero signal is the DPV response of the immunosensor incubated with 3 μL GOD/AuNPs/GO-CLB and 7 μL PBS without free CLB, and R was determined by 8 replica experiments. Compared with other methods (as shown in Table 1), this immunosensor possesses a lower detection limit and wider detection range than most of other detection methods.

The intra-assay precision of the immunosensor was evaluated by detection of CLB at two levels for five replicative measurements. The intra-assay variation coefficients (CV) were 3.1% and 6.8% at CLB concentrations of 10 and 500 ng/mL, respectively, indicating a satisfactory repeatability. In addition, the inter-assay variation coefficients at these concentrations for five different immunosensors were 7.7% and 8.9% respectively, showing acceptable fabrication reproducibility. When the immunosensor was not in use, it was stored in refrigeratory at 4 °C. 93.5% of the initial response is obtained after 1 month, reflecting a relatively good stability.

To evaluate the specificity of this immunosensor, β-agonists, such as ractopamine, dobutamine and salbutamol were chosen as interferes. The current responses of each of the interferes and CLB of the same concentration (500 ng/mL) as well as blank solution were investigated. Then the percentages of inhibition were calculated as 76.2 ± 0.8%, 2.97 ± 0.08%, 6.52 ± 0.15%, 4.9 ± 0.13%

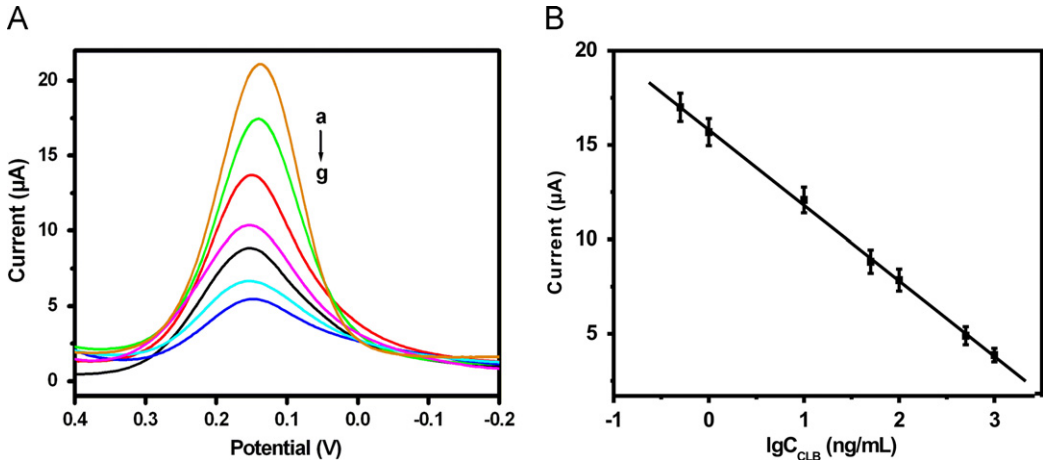

Fig. 5. (A) Typical DPV of competitive immunosensor using GOD/AuNPs/GO-CLB bioconjugate as probe with increasing CLB from a to h (0, 0.5, 1, 10, 50, 100, 500, 1000 ng/mL) in pH 6.5 PBS containing 10 mM glucose. (B) Calibration curve of the immunosensor for CLB determination plotted on a semi-log scale. Error bars represent the standard deviation of $n=8$.

Table 1
Comparison of linear ranges and detection limits of CLB obtained by different methods.

Technique	Linear range (ng/mL)	Detection limit (ng/mL)	Reference
Electrochemical immunosensor with GO as a nanocarrier	0.5–1000	0.25	This work
Liquid chromatography with electrochemical detection	1.9–60.2	1.2	[50]
Liquid chromatography with mass spectrometry detection	0.2–10	0.1	[51]
Capillary electrophoresis immunoassay with chemiluminescence detection	1.56–12.52	0.375	[52]
Capillary electrophoresis with amperometric detection	10–500	2.4	[53]
Gas chromatography with MS capillary	0.6–19.6	–	[54]
Electrochemical method	20–4000	10	[55]
Immunosensor with surface Plasmon resonance	0.0001–0.1	0.0001	[56]
Colorimetric detection	649–1664	200	[57]
HRP-labeled elecrochemical immunosensor	0.1–10	0.1	[17]
Label-free electrochemical immunosensor	0.8–1000	0.32	[16]

Table 2
The concentrations of CLB in feed samples and coefficient variation (CV) of each response for obtaining calibration curve ($n=8$).

Concentrations (mg/kg)	0.05	0.1	1	5	10	50	100
CV (%)	4.8	5.0	4.7	5.1	5.3	5.5	5.3

Table 3
Determination of CLB in swine feed samples.

Amount added (mg/kg)	**Found (mg/kg)**	**Recovery** (%)	**RSD** (%) ($n=3$)
10	10.32	103.2	6.5
20	20.19	101.0	7.1
40	38.26	95.7	4.3
50	52.35	104.5	5.6

for CLB, ractopamine, dobutamine and salbutamol respectively ($n=5$). Therefore, other agonists do not affect the detection of CLB, indicating that the immunosensor has a good selectivity to CLB and is very suitable for the detection of CLB in real samples.

3.6. Sample analysis

A commercial feed sample was employed to assess the accuracy of the immunosensor in real matrixes. No voltammetric response corresponding to CLB was observed for the unspiked sample. According to the method of real sample preparation, the relationship between the concentration of CLB (mg/kg) in the sample and the current response (μA) follows the equation: $i\,(\mu A) = 11.80 - 3.99 \log C_{CLB}\,(mg/kg) + (R^2 = 0.997)$ with the linear range from 0.05 mg/kg to 100 mg/kg and the low detection limit is 0.025 mg/kg. The concentrations of CLB in the sample and CV of each response in the standard curve are shown in Table 2. The recovery study was performed by spiking blank swine feed samples with CLB (10, 20, 40, 50 mg/kg, $n=3$). The recovery for the CLB is varied over the range of 95.7–104.5% and the statistical results are summarized in Table 3.

4. Conclusion

A novel electrochemical immunosensor for CLB is developed based on the competitive immune-reaction. The synthesis of GOD/AuNPs/GO labeled CLB was performed by one-pot assembly of GOD and CLB on AuNPs decorated GO. In this system, GOD/AuNPs/GO-CLB competes with CLB in solution, and the electrochemical signal is dually amplified due to the GOD directed enzymatic reaction through PB-mediated electron transfer. This electrochemical immunosensor shows a good performance for detection of CLB with wide linear range from 0.5 to 1000 ng/mL and a low detection limit of 0.25 ng/mL. The satisfactory sensitivity, selectivity, stability, reproducibility and accuracy all indicate the method has a promising application in food and environmental monitoring.

Acknowledgments

This work was supported by the National Natural Science Foundation of China (No. 21175046), New Century Excellent Talents in University (No. NCET-09-0357) and Open Foundation of Shanghai Key Laboratory of Green Chemistry and Chemical Process.

References

[1] C. ópez-Erroz, P. Vi˜nas, F.J. Cerdán, M. Hernández-Córdoba, Talanta 53 (2000) 47–53.
[2] G. Brambilla, T. Cenci, F. Franconi, R. Galarini, A. Macri, F. Rodoni, M. Strozzi, A. Loizzo, Toxicol. Lett. 114 (2000) 47–53.
[3] N.J. Engeseth, K.O. Lee, W.G. Bergen, J. Food Sci. 57 (1992) 1060–1062.
[4] F. Li, Y. Feng, C. Zhao, P. Li, B. Tang, Chem. Commun. 48 (2012) 127–129.
[5] J.F. Martinez-Navarro, Lancet 336 (1990) 1311.
[6] C. Pulce, D. Lamaison, G. Keck, J. Bostvironnois, Vet. Hum. Toxicol. 33 (1991) 480.
[7] P.A. Guy, M.C. Savoy, R.H. Stadler, J. Chromatogr. B 736 (1999) 209–219.
[8] B.M. Liu, H.Y. Yan, F.X. Qiao, J. Chromatogr. B 879 (2011) 90–94.
[9] I.K. Abukhalaf, D.A. Deutsch, B.A. Parks, L. Wineski, D. Paulsen, Biomed. Chromatogr. 14 (2000) 99–105.
[10] L.M. He, Y.J. Su, Z.L. Zeng, Y.H. Liu, X.H. Huang, Anim. Food Sci. Technol. 132 (2007) 316–323.
[11] Y.C. Chen, W. Wang, J. Duan, H. Chen, Electroanalysis 17 (2005) 706–712.
[12] M.A. Johansson, K.E. Hellenas, Int. J. Food Sci. Technol. 39 (2004) 891–898.
[13] A. Posyniak, J. Zmudzki, J. Niedzielska, Anal. Chim. Acta 483 (2003) 61–67.
[14] M.A. Johansson, K.E. Hellenas, Food Agric. Immunol. 15 (2003) 197–205.
[15] L.J. Gao, N. Gan, F.T. Hu, Adv. Mater. Res. 217 (2011) 1793–1796.
[16] P.L. He, Z.Y. Wang, L.Y. Zhang, Food Chem. 112 (2009) 707–714.
[17] G. Liu, H. Chen, H. Peng, Biosens. Bioelectron. 28 (2011) 308–313.
[18] P. Hazarika, B. Ceyhan, C.M. Niemeyer, Small 1 (2005) 844–848.
[19] G. Liu, Y. Lin, Talanta 74 (2007) 308–317.
[20] R.J. Cui, C. Liu, J.M. Shen, Adv. Funct. Mater. 18 (2008) 2197–2204.
[21] J. Wang, G.D. Liu, M.H. Engelhard, Anal. Chem. 78 (2006) 6974–6979.
[22] G. Lai, F. Yan, H. Ju, Anal. Chem. 81 (2009) 9730–9736.
[23] X. Yu, B. Munge, V. Patel, G. Jensen, A. Bhirde, J.D. Gong, S.N. Kim, J. Gillespie, J.S. Gutkind, F. Papadimitrakopoulos, J.F. Rusling, J. Am. Chem. Soc. 128 (2006) 11199–11205.
[24] D. Du, Z.X. Zou, Y. Shin, J. Wang, H. Wu, M.H. Engelhard, J. Liu, I.A. Aksay, Y.H. Lin, Anal. Chem. 82 (2010) 2989–2995.
[25] Y.F. Wu, C.L. Chen, S.Q. Liu, Anal. Chem. 81 (2009) 1600–1607.
[26] V. Mani, B.V. Chikkaveeraiah, V. Patel, J.S. Gutkind, J.F. Rusling, ACS Nano 3 (2009) 585–594.
[27] M. Du, T. Yang, K. Jiao, J. Mater. Chem. 20 (2010) 9253–9260.
[28] A.M. Jiaul Haque, H. Park, D. Sung, S.Y. Jon, S.Y. Choi, K. Kim, Anal. Chem. 83 (2012) 746–752.
[29] X.L. Li, X.R. Wang, L. Zhang, S. Lee, H.J. Dai, Science 319 (2008) 1229–1232.
[30] Z. Liu, J.T. Robinson, X. Sun, H.J. Dai, J. Am. Chem. Soc. 130 (2008) 10876–10877.
[31] X.M. Sun, Z. Liu, K. Welsher, J.T. Robinson, A. Goodwin, S. Zaric, H.J. Dai, Nano Res. 1 (2008) 203–212.
[32] X.Y. Yang, X.Y. Zhang, Z.F. Liu, Y.F. Ma, Y. Huang, Y.S. Chen, J. Phys. Chem. C 112 (2008) 17554–17558.
[33] L.M. Zhang, J.G. Xia, Q.H. Zhao, L.W. Liu, Z.J. Zhang, Small 6 (2010) 537–554.
[34] D. Du, L.M. Wang, Y.Y. Shao, J. Wang, M.H. Engelhard, Y.H. Lin, Anal. Chem. 83 (2011) 746–752.
[35] B.Y. Wu, S.H. Hou, F. Yin, Z.X. Zhao, Y.Y. Wang, X.S. Wang, Q. Chen, Biosens. Bioelectron. 22 (2007) 2854–2860.
[36] I. Izquierdo-Lorenzo, S. Sanchez-Cortes, J.V. Garcia-Ramos, Langmuir 26 (2010) 14663–14670.
[37] H. Xu, L.P. Zeng, S.J. Xing, G.Y. Shi, Y.Z. Xian, L.T. Jin, Electrochem. Commun. 10 (2008) 1839–1843.
[38] W. Hummers, R. Offeman, J. Am. Chem. Soc. 80 (1958) 1339.
[39] K.P. Liu, J.J. Zhang, C.M. Wang, J.J. Zhu, Biosens. Bioelectron. 26 (2011) 3627–3632.
[40] S.Y. Wang, D.S. Yu, L.M. Dai, D.W. Chang, J.B. Baek, ACS Nano 5 (2011) 6202–6209.
[41] B. Li, X.T. Zhang, X.H. Li, Chem. Commun. 46 (2010) 3499.
[42] Q.M. Ji, S. Acharya, J.P. Hill, G.J. Richards, Adv. Mater. 20 (2008) 4027.
[43] G. McGrath, W.F. Smyth, J. Chromatogr. B 681 (1996) 125–131.
[44] C. Guarise, L. Pasquato, P. Scrimin, Langmuir 21 (2005) 5537–5541.
[45] K.G. Thomas, S. Barazzouk, B.I. Ipe, S.T.S. Joseph, P.V. Kamat, J. Phys. Chem. B 108 (2004) 13066–13068.
[46] W. Zhao, J.J. Xu, C.G. Shi, H.Y. Chen, Langmuir 21 (2005) 9630–9634.
[47] Y.Q. Lin, K. Liu, P. Yu, L. Xiang, X.C. Li, L.Q. Mao, Anal. Chem. 79 (2007) 9577–9583.
[48] X.Y. Wang, H.F. Gu, F. Yin, Y.F. Tu, Biosens. Bioelectron. 24 (2009) 1527–1530.
[49] S. Chen, R. Yuan, Y.Q. Chai, Y. Xu, L. Min, N. Li, Sens. Actuators B 135 (2008) 236–244.
[50] X.Z. Zhang, Y.R. Gan, F.N. Zhao, Anal. Chim. Acta 489 (2003) 95–101.
[51] C. Juan, C. Igualada, F. Moragues, N. León, J. Ma˜nes, J. Chromatogr. A 1217 (2010) 6061–6068.
[52] B.L. Su, D.P. Tang, J. Tang, Y.L. Cui, G.N. Chen, Biosens. Bioelectron. 30 (2011) 229–234.
[53] L. Zhao, J. Zhao, W.G. Huangfu, Y.L. Wu, Chromatographia 72 (2010) 365–368.
[54] G.J. McGrath, E. O Kane, W.F. Smyth, F. Tagliaro, Anal. Chim. Acta 322 (1996) 159–166.
[55] X. Fan, S.P. Xie, Z.S. Zheng, J. Mol. Liq. 169 (2012) 102.
[56] G.C. Zhu, Y.J. Hu, J. Gao, L. Zhong, Anal. Chim. Acta 697 (2011) 61–66.
[57] P.L. He, L. Shen, R.Y. Liu, Z.P. Luo, Z. Li, Anal. Chem. 83 (2011) 6988–6995.